Plant Cell Tiss Organ Cult (2013) 115:85–97
DOI 10.1007/s11240-013-0343-x

ORIGINAL PAPER

Morphological, physiological and oxidative stress markers during acclimatization and field transfer of micropropagated *Tuberaria major* plants

M. L. Osório · S. Gonçalves · N. Coelho · J. Osório · A. Romano

Received: 17 January 2013 / Accepted: 15 June 2013 / Published online: 23 June 2013

Abstract *Tuberaria major* (Willk.) P. Silva and Rozeira is a critically-endangered rock rose species endemic to Portugal. Because the species needs to be preserved, this study evaluated the morphological and physiological traits of micropropagated *T. major* plants during acclimatization and field transfer. There were no significant differences between wild and micropropagated plants in the field, although the latter underwent significant changes during acclimatization. Leaf pubescence and leaf mass per area increased during acclimatization whereas the chlorophyll content and chlorophyll/carotenoid ratio declined to eventually match those of wild plants. Stomatal conductance (g_s) and transpiration rates (E) also declined substantially during acclimatization, thus preventing uncontrolled wilting. Photosynthetic rate (P_N) was initially negative but increased during the later stages of acclimatization. Maximum quantum yield of PSII (F_v/F_m) remained constant at 0.78–0.85, showing that the plants were healthy and unstressed. PSII quantum efficiency (ϕ_{PSII}) was initially low but increased during acclimatization along with photosynthetic performance as the energy partitioning in PSII was adjusted. This was balanced by the decline in non-regulated energy dissipation (ϕ_{NO}) from an initially high value. Electrolyte leakage and malondialdehyde content remained constant at similar levels in both groups of plants, but H_2O_2 levels were higher in the field, perhaps indicating the early induction of antioxidant defense systems. The present study shows that *T. major* has enough phenotypic plasticity to adapt to changing environments and that the procedure described herein can be used for the restoration and preservation of this species.

Keywords Acclimatization · Electrolyte leakage · Energy partitioning · Hydrogen peroxide · Photosynthesis · Lipid peroxidation

Introduction

Plants cultivated in vitro experience significant stress when exposed to the extreme conditions of the culture medium (high levels of sucrose and nitrogen) and microenvironment (low-intensity light, high humidity and limited gas exchange) resulting in dramatic morphological and physiological changes (Pospíšilová et al. 1999; Hazarika 2006; Preece 2010). Once adapted to these in vitro conditions, the plantlets experience further stress when transferred to the greenhouse or field because they are switched to higher-intensity light and lower humidity, requiring the rapid development of survival mechanisms based on environmentally-induced shifts in phenotype. The ability to modify the phenotype and its underlying metabolism in response to environmental changes is known as phenotypic plasticity (Nicotra et al. 2010). Understanding the morphological and physiological responses that allow plants to acclimatize in new environments can help to improve the performance and survival of micropropagated plants (Brito et al. 2009). The comparison of micropropagated and seed-derived plants in the field is also necessary to ensure that micropropagated plants can adapt to survive in their natural environment (Osório et al. 2012).

M. L. Osório (✉) · S. Gonçalves · N. Coelho · A. Romano
Faculty of Sciences and Technology, IBB-CGB, University of Algarve, Campus de Gambelas, 8005-139 Faro, Portugal
e-mail: mlosorio@ualg.pt

J. Osório
Faculty of Sciences and Technology, ICAAM, University of Algarve, Campus de Gambelas, 8005-139 Faro, Portugal

Tuberaria major (Willk.) P. Silva and Rozeira is a critically-endangered rock rose species (Cistaceae) endemic to the Algarve region of southern Portugal. The species was formerly distributed throughout the Algarve coastal region, but today it is confined to a few isolated and sun-exposed sandy pockets, reflecting a long history of natural and anthropogenic disturbances (ICN 2006; Bilz 2011). The urgent restoration and preservation of this species is required. The preservation of germplasm can increase the number of individuals in natural populations, and cryopreservation can be used to conserve seeds. An efficient *T. major* micropropagation protocol has recently been described (Gonçalves et al. 2009, 2010) but it is also necessary to evaluate how micropropagated plants acclimatize in the field in order to ensure that the method is suitable for restoration and preservation. A study was therefore carried out to compare the morphological and physiological characteristics of micropropagated *T. major* plants and wild (seed-derived) plants in their natural habitat, including the analysis of survival, growth, relative water content, leaf mass per area, gas exchange, chlorophyll fluorescence, leaf pigment levels, H_2O_2 levels, lipid peroxidation and electrolyte leakage throughout acclimatization. Six weeks after transfer to the field, the same traits were measured in the micropropagated and wild plants to monitor their performance under field conditions. The potential of this micropropagation technique for the restoration of depleted natural populations of endangered species is discussed.

Materials and methods

Plant material and acclimatization conditions

Tuberaria major plantlets were produced in vitro according to a recently-developed protocol (Gonçalves et al. 2010). Cultures were initiated by germinating in vitro seeds collected from a natural population at Campus de Gambelas, Faro, in the Algarve region of southern Portugal. Shoots were multiplied on MS medium (Murashige and Skoog 1962) supplemented with 0.2 mg l^{-1} zeatin, and were subcultured at 6-week intervals. Roots were induced from individual shoots cultivated for 6 weeks in half-strength MS medium. The cultures were maintained at 25 ± 2 °C with a 16-h photoperiod (cool white fluorescent lamps, 69 µmol m^{-2} s^{-1}).

Rooted plantlets were transferred to 350-ml plastic pots containing a 3:1 (v/v) mixture of peat and vermiculite, and were maintained for 6 weeks in a growth chamber (500E, Aralab, Lisboa, Portugal) under controlled conditions [25 ± 2 °C, 16-h photoperiod, photosynthetic photon flux density (PPFD) 100 µmol m^{-2} s^{-1}]. The relative humidity was initially 98 % but was reduced during the acclimatization period to reach 70 % during the final week. The plantlets were watered twice weekly with a 12:4:6 NPK solution including essential micronutrients. The plants were subsequently transferred to large pots containing peat and vermiculite as above and were cultivated in an open greenhouse without environmental conditioning for 6 weeks. The relative humidity varied from 50 to 60 % and the maximum PPFD was 200–400 µmol m^{-2} s^{-1}. The acclimatized plants were transferred to the field among a natural population of *T. major* at Campus de Gambelas. The local wild plants were used as controls. This region has an arid climate (hot dry summer with mean high temperatures ~30 °C), an annual rainfall of 400–500 mm and a PPFD of 1,700–1,900 µmol m^{-2} s^{-1} at midday. Measurements were taken 6 weeks after planting.

Plant growth and leaf characteristics

The number of new leaves produced during each acclimatization period and the length of the most recent fully-expanded leaf were evaluated (n = 10) and the survival rates were estimated. Leaf mass per area (LMA) was calculated as the ratio of dry mass (DM), determined after drying at 63 °C until constant mass was achieved, to the leaf area (LA) according to the formula described by Dijkstra (1989):

$$\mathrm{LMA} = \mathrm{DM}/\mathrm{LA} = (\mathrm{FM}/\mathrm{LA}) \times (\mathrm{DM}/\mathrm{FM})$$

where FM is the fresh mass, FM/LA represents the leaf thickness and DM/FM represents the density.

Leaf gas exchange and chlorophyll fluorescence imaging

Stomatal conductance was measured for water vapor diffusion (g_s), net CO_2 uptake rate (P_N), transpiration rate (E) and intercellular CO_2 concentration (C_i) using a portable gas exchange measuring system (HCM-1000, H. Walz, Effeltrich, Germany). Measurements were taken from the youngest fully-expanded leaf at the end of each acclimatization period, during the middle of the light period when the photosynthetic photon flux density was 150–200 µmol m^{-2} s^{-1}, the relative air humidity was ~45 %, the air temperature was 20 °C, and the ambient CO_2 concentration was 330–350 µmol mol^{-1} air at a flow rate of 800 cm^3 min^{-1}.

Chlorophyll fluorescence was assessed in the leaves used to measure gas exchange (see above) using a mini blue version of the Imaging-PAM Chl fluorometer (IMAG-MIN/B, Walz, Effeltrich, Germany) after 20 min of darkness. In order to evaluate spatial and temporal heterogeneity, three areas of interest were selected and images of F_0

were obtained by applying measuring light pulses modulated at 1 Hz. Images of maximum fluorescence yield (F_m) were obtained using a saturating blue pulse (800 ms) with an intensity of 6,000 μmol m^{-2} s^{-1} PPFD at 10 Hz, and images of F_v/F_m were thus derived. After switching to actinic illumination (134 μmol photons m^{-2} s^{-1}), saturating pulses were applied at 20-s intervals for 5 min in order to determine the maximum fluorescence yield (F_m') and the Chl fluorescence yield (F_s) during illumination. The actual PSII quantum efficiency (ϕ_{PSII}) and the coefficient of photochemical quenching (q_p) were calculated as described by Genty et al. (1989). Quantum yields of regulated (ϕ_{NPQ}) and of non-regulated (ϕ_{NO}) energy dissipation in PSII were calculated as described by Kramer et al. (2004). F_0' value was estimated using the approximation of Oxborough and Baker (1997). PSII electron transport rate (ETR) was calculated as $\phi_{PSII} \times PPFD \times 0.5 \times 0.84$, using a leaf absorbance of 0.84 because that is the most common value for C_3 plants (Björkman and Demmig 1987). The steady-state chlorophyll fluorescence parameter $1 - q_p$ (also known as the PSII excitation pressure) was also measured to estimate the relative reduction state of QA, the first stable quinone electron acceptor of PSII.

The relationships between photosynthetic efficiency and incident photosynthetic photon flux density (PPFD) were measured by recording rapid light curves (RLCs) after each chlorophyll fluorescence kinetics measurement, by exposing leaves to a sequence of actinic pulses (0–700 μmol photons m^{-2} s^{-1}) in 12 discrete PPFD steps, each lasting 10 s. Images of F and F_m' were acquired at the end of each illumination step, from which images of fluorescence parameters were calculated automatically using Imaging Win software. Light curves were constructed by averaging the data from three selected areas of interest in the corresponding images obtained from five plants per treatment.

Leaf pigments and total soluble protein

Photosynthetic pigments were analyzed in 2.0-cm^2 samples of freeze-dried leaf tissue extracted in 100 % acetone and measured in a spectrophotometer (Shimadzu UV-160, Kyoto, Japan) at 661.6, 644.8 and 470 nm. The levels of chlorophylls and carotenoids were estimated as described by Lichtenthaler (1987).

Anthocyanins were extracted from 2.0-cm^2 leaf discs in 1:99 (v/v) HCl-acidified methanol and incubated at 4 °C for 4 h to avoid the degradation of chlorophylls, whose products would interfere with the absorbance of anthocyanins at 530 nm. After clearing by centrifugation at 10,000×*g* for 30 min, the optical density of the supernatant was scanned between 400 and 700 nm and anthocyanin levels were measured as described by Mancinelli (1984) using $OD_{530} - 0.25 \times OD_{657}$ to account for chlorophyll interference. The anthocyanin content was calculated based on cyanidin-3-glucoside using 29,600 l mol^{-1} cm^{-1} as the extinction coefficient and 445 g mol^{-1} as the molecular weight. The total soluble protein levels were determined as described by Bradford (1976) using bovine serum albumin as a standard.

Hydrogen peroxide content

The H_2O_2 content was determined as described by Loreto and Velikova (2001). Fresh plant material (100 mg) was homogenized in 1 ml 0.1 % (w/v) trichloroacetic acid (TCA) at 4 °C. The homogenate was centrifuged at 12,000×*g* for 15 min and 0.2 ml of the supernatant was added to 0.2 ml 10 mM potassium phosphate buffer (pH 7.0) and 0.4 ml 1 M KI. The reaction was developed for 30 min in darkness and the H_2O_2 content was determined at 390 nm against a set of H_2O_2 standards. The results were expressed as μmol g^{-1} fresh mass (FM).

Lipid peroxidation and electrolyte leakage

Oxidative damage to lipids was evaluated by measuring lipid peroxidation, which was determined by the amount of malondialdehyde (MDA) available to react with 2-thiobarbituric acid (TBA) (Hodges et al. 1999). The MDA concentration was expressed in terms of μmol g^{-1} FM, using an extinction coefficient of 155 mM^{-1} cm^{-1} at 532 nm. Absorbance was measured at 600 and 440 nm to allow for interference due to nonspecific turbidity and carbohydrates.

Electrolyte leakage (EL) was measured to evaluate membrane permeability using an electrical conductivity meter as described by Lutts et al. (1996). Fresh plant material (100 mg) was washed three times with distilled water to remove surface contamination. The samples were cut into 1-cm^2 segments and incubated in distilled water overnight at 25 °C in a rotary shaker. The electrical conductivity (EC_1) of the bathing solution was recorded. The samples were then boiled for 30 min to release all electrolytes, cooled to 25 °C and the final electrical conductivity (EC_2) was measured. EL was calculated using the formula $EL = (EC_1/EC_2) \times 100$.

Statistical analysis

Statistical analysis was carried out using SPSS v16.0.1 and presented using SigmaPlot v10.00 (SPSS Inc., Chicago, IL). Data were processed by one-way ANOVA after testing for normality and homogeneity of variance. If the ANOVA yielded a significant F value ($P < 0.05$), the individual means of treatments were compared using the Student–Newmans–Keuls post hoc test. Values are presented as

Fig. 1 **a** A population of *T. major* plants at Campus de Gambelas, from where the original seeds were collected; **b** a *T. major* flowering plant; **c** micropropagated plants during acclimatization; **d**, **e** micropropagated plants during field transfer; **f** field plants 6 weeks after transfer. *Blue arrows* indicate micropropagated plants and *red arrows* indicate wild plants. (Color figure online)

means ± standard errors of ten replicates for growth parameters and five replicates for the other experiments.

Results

Survival rates, growth and leaf characteristics

Plantlets regenerated in vitro were successfully acclimatized in the growth chamber (88 % survival) and then in the greenhouse (84 % survival). The global survival rate during acclimatization from in vitro growth to field transfer was 74 %. The surviving plants were used to establish the field trial with 100 % success (Fig. 1). After 6 weeks in the field, the regenerated plants appeared healthy and uniform in growth.

The mean number of new leaves per plant decreased during the final stage of acclimatization, but the leaf length increased significantly ($P < 0.05$) in this stage reaching a similar length to the leaves of wild plants (Table 1). Leaves from plants in the field (wild and regenerated) had a significantly higher ($P < 0.05$) leaf mass per area (LMA) than in vitro, growth chamber and greenhouse plants, although LMA was highest overall in the wild plants. The fresh mass/foliar area ratio (FM/LA) was similar throughout acclimatization but was significantly lower than in wild plants ($P < 0.05$). The dry mass/fresh mass ratio (DM/FM) of both wild and regenerated plants was similar, and in each case was significantly lower than other acclimatization stages (Table 1). It was also clear that the leaf hair density (pubescence) increased under field conditions.

Leaf gas exchange

Leaf gas exchange data are summarized in Fig. 2a–d. Stomata were completely open during in vitro cultivation ($g_s = 595$ mmol m^{-2} s^{-1}) but began to close during acclimatization in the growth chamber, reducing the stomatal conductance (g_s) by up to tenfold in the greenhouse plants. There were no further significant changes in g_s between the greenhouse and field plants (regenerated or wild). The changes in g_s were matched by a parallel reduction in transpiration rate (E). The micropropagated plants were characterized by negative photosynthetic rates (P_N) in vitro, reflecting a negative balance between photosynthesis and respiration (dark plus photorespiration rates). Six weeks after transfer to the growth chamber, P_N increased and C_i decreased significantly ($P < 0.05$). There were no significant differences ($P \geq 0.05$) between P_N and C_i values of plants in the growth chamber, greenhouse and field, although C_i value of the greenhouse plants was marginally lower.

Table 1 Morphological traits of wild and micropropagated *T. major* plants during rooting (in vitro) and acclimatization (growth chamber, greenhouse and field)

Stages	New leaves (N°)	Leaf length (cm)	LMA (g m^{-2})	FM/LA (g m^{-2})	DM/FM (g g^{-1})
In vitro	11.2 ± 1.9a	4.4 ± 0.2c	58.6 ± 3.0c	306.3 ± 12.5b	0.193 ± 0.012b
Growth chamber	13.0 ± 1.8a	6.3 ± 0.3b	59.1 ± 2.9c	324.8 ± 12.5b	0.182 ± 0.008b
Greenhouse	7.6 ± 1.4b	9.1 ± 0.4a	36.5 ± 5.3c	281.5 ± 21.9b	0.118 ± 0.017c
Field	8.1 ± 1.4b	8.4 ± 0.5a	163.9 ± 20.9b	379.2 ± 57.1b	0.390 ± 0.003a
Wild plants	8.0 ± 1.6b	8.0 ± 0.9a	213.8 ± 6.2a	476.8 ± 37.7a	0.416 ± 0.006a

Mean ± SE (n = 10) within each column with different letters are significantly different ($P < 0.05$) according to the SNK test

LMA leaf mass per area, *FM* fresh mass, *DM* dry mass, *LA* leaf area

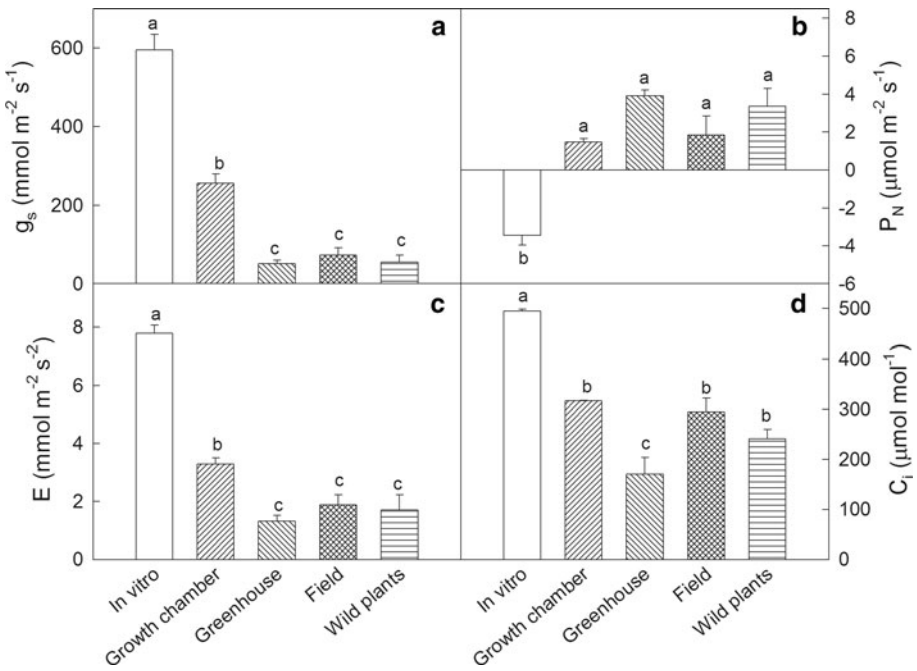

Fig. 2 Specific properties of leaves from micropropagated *T. major* plants during acclimatization and 6 weeks after field transfer, compared with wild plants. **a** Stomatal conductance (g_s); **b** photosynthetic rate (P_N); **c** transpiration rate (E); **d** intercellular CO_2 concentration. Data represent mean ± SE (n = 5), and *different letters* show significant differences ($P < 0.05$) according to the SNK test

Quantitative analysis of chlorophyll fluorescence

Fluorescence imaging was used to monitor changes in Chl fluorescence and detect heterogeneity as a response to environmental challenges associated with acclimatization. As shown in Fig. 3, the maximum photochemical efficiency of PSII (F_v/F_m) remained homogeneous during acclimatization, with mean values close to maximum (0.78–0.85). Although there was no significant difference in F_v/F_m between acclimatization stages, there was a significant reduction in F_m and F_0 (~55 %) in field plants (regenerated and wild) relative to plants at the other acclimatization stages (data not shown).

The model described by Kramer et al. (2004) was used to determine the partitioning of PSII excitation energy flux between three different pathways, i.e. photochemical utilization, regulated energy dissipation (a protective loss process) and non-regulated energy dissipation (a loss process reflecting PSII inactivity). These three fluxes are described by the quantum yields ϕ_{PSII}, ϕ_{NPQ} and ϕ_{NO}, respectively, and add up to unity. Color-coded images of representative individual leaves captured at PPFD 134 µmol m^{-2} s^{-1} were used to confirm that ϕ_{PSII}, ϕ_{NPQ} and ϕ_{NO} remained generally homogeneous along the leaf (Fig. 3), but that quantitative differences could be detected during acclimatization (Fig. 4). Quantum yield of PSII photochemistry (ϕ_{PSII}) increased progressively during acclimatization and reached the level characteristic of wild plants during the greenhouse stage. This increase in ϕ_{PSII} (~53 % higher than in vitro plants) was concomitant with a reduction (~34 %) in the quantum yield of non-regulated energy dissipation at PSII (ϕ_{NO}), whereas the regulated energy dissipation at PSII (ϕ_{NPQ}) did not vary (~13 %).

No changes were evident in the excitation capture efficiency of open centers (F_v'/F_m') (Fig. 5a). Excitation pressure ($1 - q_p$) declined gradually and significantly

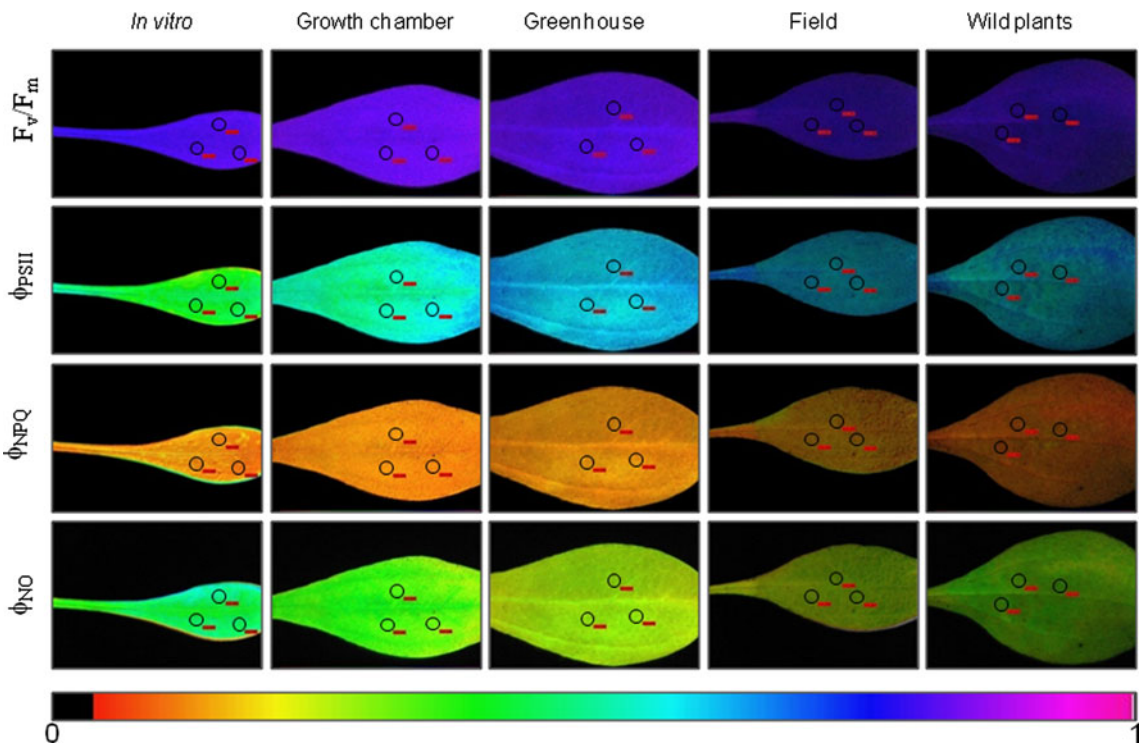

Fig. 3 Chlorophyll fluorescence images of maximum PSII photochemical efficiency in dark-adapted leaves (F_v/F_m), actual PSII quantum yield (ϕ_{PSII}), quantum yield of regulated energy dissipation of PSII (ϕ_{NPQ}) and quantum yield of non-regulated energy dissipation of PSII (ϕ_{NO}) measured at a steady-state (134 μmol m^{-2} s^{-1}) in *T. major* leaves during acclimatization and in the field. The false color code underneath the images ranges from 0.000 (*black*) to 1.000 (*pink*). For each sample leaf, three areas of interest were defined and displayed as small *circles* within each image, accompanied by a *red box* showing the averaged values of fluorescence parameters. (Color figure online)

throughout acclimatization, reaching the level characteristic of wild plants during the greenhouse stage (Fig. 5b). The fraction of open centers estimated by photochemical quenching (q_p) increased throughout acclimatization, and the decline in $1 - q_p$ was accompanied by an increase in the electron transport rate (ETR) (Fig. 5c). Non-photochemical quenching (NPQ) declined slightly in the growth chamber relative to in vitro plants, but then increased significantly ($P < 0.05$) under greenhouse and field conditions, reaching values statistically equivalent ($P \geq 0.05$) to those observed in vitro (Fig. 5d). As expected, NPQ increased with the higher light intensity throughout acclimatization (Fig. 6a), particularly under greenhouse and field conditions compared to in vitro and growth chamber plants. However, the NPQ values of greenhouse plants were similar to those found in field plants only under low light intensities (down to 450 μmol m^{-2} s^{-1}) whereas higher PPFD conditions induced lower NPQ values than field plants. The trend in the ETR response to stepwise increases in PPFD (Fig. 6b) was similar to that observed for NPQ. In contrast, the ETR values of in vitro plants were lower than those of plants in the growth chamber. Furthermore, in vitro plants showed the highest excitation pressure ($1 - q_p$) values in response to PPFD increases, whereas field plants showed the lowest (Fig. 6c). Unsurprisingly, ϕ_{PSII} declined concomitantly with the increasing PPFD throughout acclimatization and in the field (Fig. 7a). However, these changes were more dramatic in the growth chamber and in vitro, and appeared to be associated with the downregulation of ETR (Fig. 6b). The pattern of differences observed for NPQ (Fig. 6a) was mirrored by the quantum efficiency of the dissipation (ϕ_{NPQ}), although the differences were not so dramatic (Fig. 7b). In contrast to ϕ_{NPQ}, the quantum yield of non-regulated energy dissipation in PSII (ϕ_{NO}) remained constant (~ 0.25) in both wild and regenerated field plants, as well as in greenhouse plants (Fig. 7c), whereas ϕ_{NO} increased in vitro and in the growth chamber plants in response to the higher PPFD values, reaching ~ 0.52 at PPFD values up to 500 μmol m^{-2} s^{-1}.

Leaf pigments and total soluble protein

The total chlorophyll content was significantly higher in the growth chamber and greenhouse plants but there were no significant differences between in vitro plants and field plants (regenerated or wild). The carotenoid profile was similar to the total chlorophyll content, whereas the Chl/Car ratio was constant during the in vitro and acclimatization

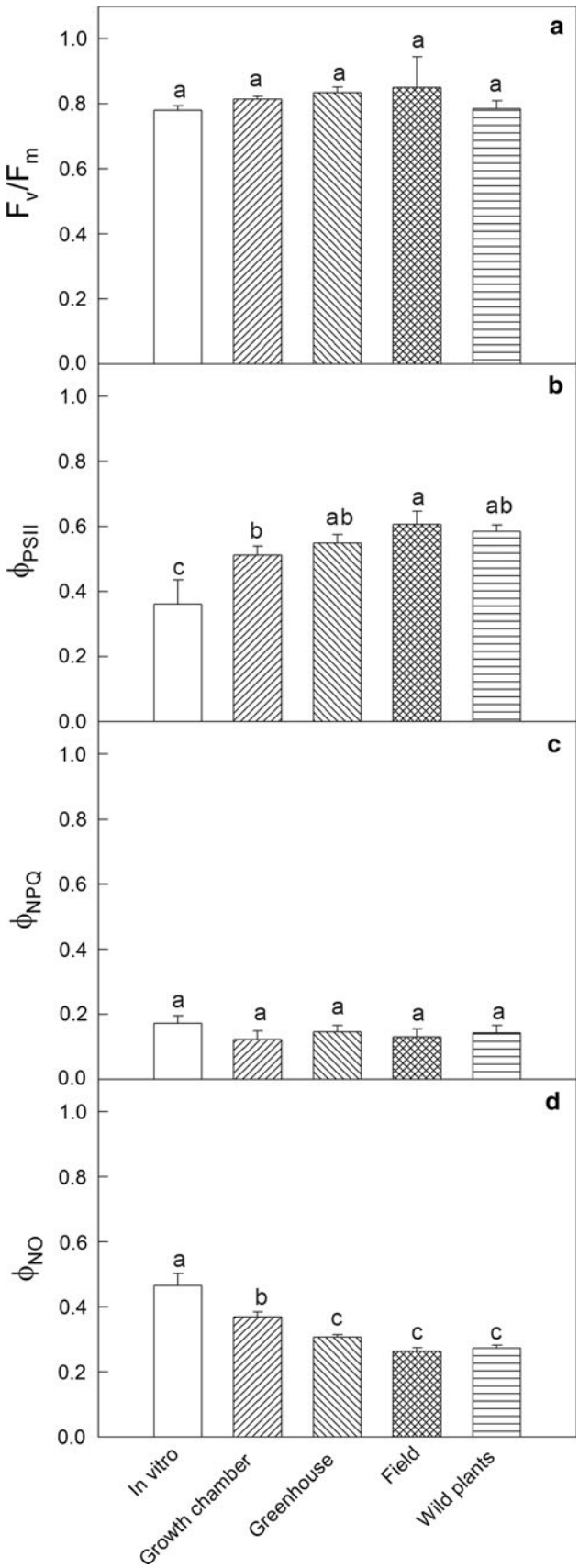

◀**Fig. 4** Quantitative analysis of imaged chlorophyll fluorescence parameters in *T. major* leaves during acclimatization and in the field. **a** Maximum PSII photochemical efficiency in dark-adapted leaves (F_v/F_m); **b** actual PSII quantum yield (ϕ_{PSII}); **c** quantum yield of regulated energy dissipation of PSII (ϕ_{NPQ}); **d** quantum yield of non-regulated energy dissipation of PSII (ϕ_{NO}) measured at a steady-state (134 μmol m^{-2} s^{-1}). Data represent mean ± SE (n = 5), and *different letters* are significantly different ($P < 0.05$) according to the SNK test

stages (growth chamber and greenhouse) but significantly lower in field plants (Table 2). There was no clear trend in the anthocyanin content (data not shown). The total soluble protein content was significantly higher ($P < 0.05$) in the in vitro plants and during the acclimatization stages than in field plants (regenerated or wild).

Hydrogen peroxide levels, electrolyte leakage, and lipid peroxidation

The H_2O_2 content remained significantly lower ($P < 0.05$) during the acclimatization stages than after transfer to the field (Fig. 8a). However, significant differences were observed between the regenerated and wild plants, the latter showing the highest levels. There were no significant differences ($P \geq 0.05$) in electrolyte leakage when we compared the in vitro, acclimatization and field stages (Fig. 8b). The lowest values for lipid peroxidation (estimated by measuring MDA production) were found in the greenhouse plants, differing significantly ($P < 0.05$) from the in vitro and field plants (Fig. 8c).

Discussion

Environmental changes can induce morphological and physiological responses in plants that allow them to adapt to novel climatic conditions. The degree of functional plasticity in different plant species is considered a crucial determinant of their ability to respond to both short-term and long-term environmental changes (Nicotra et al. 2010). However, when such changes are sudden and severe, as seen when plants are propagated in vitro and then transferred directly to the field, some species are unable to acclimatize to the adverse conditions and therefore die. A series of gradual changes in environmental conditions is required before field transfer in such cases, especially to prevent desiccation and photo-inhibition.

Although the 74 % survival rate achieved for *T. major* plants at the end of the acclimatization process seems low, this is similar to the results reported for other species (Huang and Dai 2011; Yang et al. 2012; Raju et al. 2013) including endangered Cistaceae (López et al. 2006). The

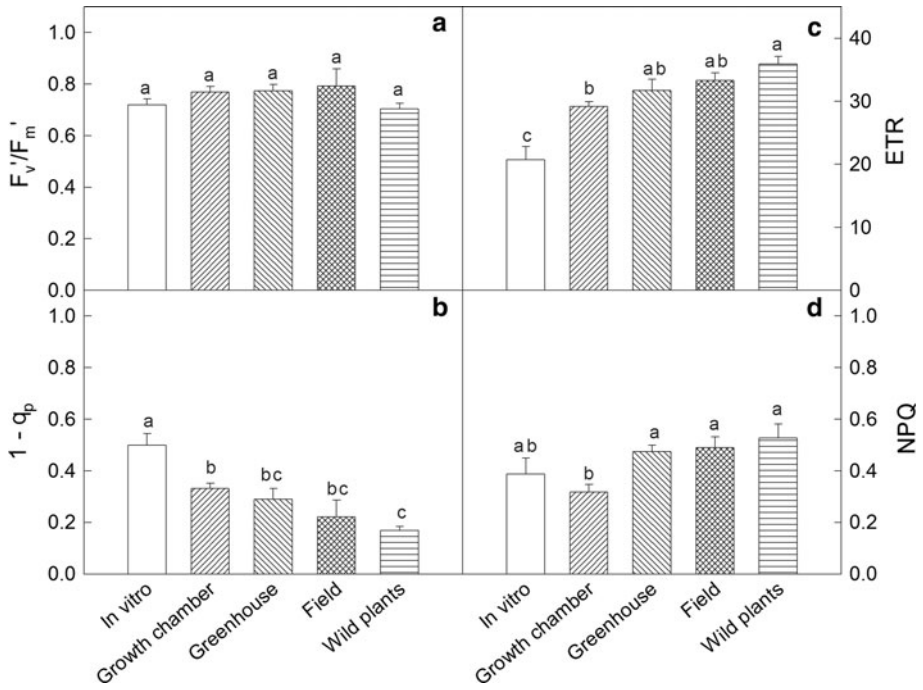

Fig. 5 Specific properties of *T. major* leaves during acclimatization and in the field. **a** Excitation capture efficiency of open centers F_v'/F_m'; **b** excitation pressure ($1 - q_p$); **c** electron transport rate (ETR); **d** non-photochemical quenching (NPQ) measured at a steady-state (134 μmol m^{-2} s^{-1}). Data represent mean ± SE (n = 5), and *different letters* are significantly different ($P < 0.05$) according to the SNK test

data also show that micropropagated *T. major* plants benefit from a period of acclimatization in the growth chamber and greenhouse because a 100 % of survival rate was achieved in the field, and the field plants performed similarly to wild plants growing in the same location (Fig. 1). The acclimatized field plants showed active growth without senescence and no significant morphological or physiological differences were found between regenerated and wild plants. This reflects the gradual acclimatization process, which triggered changes necessary for survival and the maintenance of normal growth under field conditions (Pospíšilová et al. 1999; Hazarika 2006).

The production of new leaves continued throughout acclimatization and the rate was approximately the same in the field as that in wild plants (Table 1). The leaf structure also changed when the regenerated plants were transferred to the field, as evidenced by their higher LMA (similar to that of wild plants) compared to the earlier acclimatization stages (Table 1). By separating LMA into its components (Dijkstra 1989), it was shown that the increase resulted more from changes in leaf density (morphological and anatomical changes) than thickness (fresh weight or cellular volume). The increased investment in structural tissues underlying this phenomenon would clearly enhance the resistance of regenerated plants to adverse environmental conditions (Chaves et al. 2003). Another adaptive trait visible in both the regenerated and wild plants was the development of leaf hairs. Leaf pubescence may increase the thickness of the leaf boundary layer, thus reducing the rate of water loss and also absorbance, limiting the leaf temperature and transpiration rate (Ehleringer and Mooney 1978).

Following field transfer, total chlorophyll content and Chl/Car ratio in the regenerated plants declined to values similar to those of wild plants (Table 2). The loss of chlorophyll reduces the P_N value, and is hence considered a negative stress response. However, plants growing under Mediterranean conditions are often exposed to excess excitation energy, so the loss of chlorophyll may also represent an adaptive response to light stress (Kyparissis et al. 1995; Munné-Bosch and Alegre 1999). This reduces the amount of light intercepted by the leaves, thus limiting further damage to the photosynthetic machinery caused by the formation of activated oxygen under strong light. A low or declining Chl/Car ratio may also indicate an increase in photoprotection because carotenoids facilitate the non-radiative dissipation of excitation energy and thus increase antioxidant protection (Demmig-Adams 1998). The total chlorophyll and carotenoid levels and the Chl/Car ratio were similar in wild and regenerated plants in the field, supporting the conclusion that the micropropagated plants were well adapted to field conditions.

The in vitro plantlets displayed negative net photosynthesis rates (Fig. 2b), thereby revealing an unfavorable balance between photosynthesis and respiration. However, new leaves produced during acclimatization showed higher P_N values, particularly during the greenhouse stage, and the value remained steady under field conditions. Gradually improving photosynthetic competence during acclimatization has been observed in several other plant species regenerated in vitro (Amâncio et al. 1999; Guan et al. 2008; Siddique and Anis 2008). In *T. major*, the increase in P_N appears to be unrelated to changes in stomatal behavior,

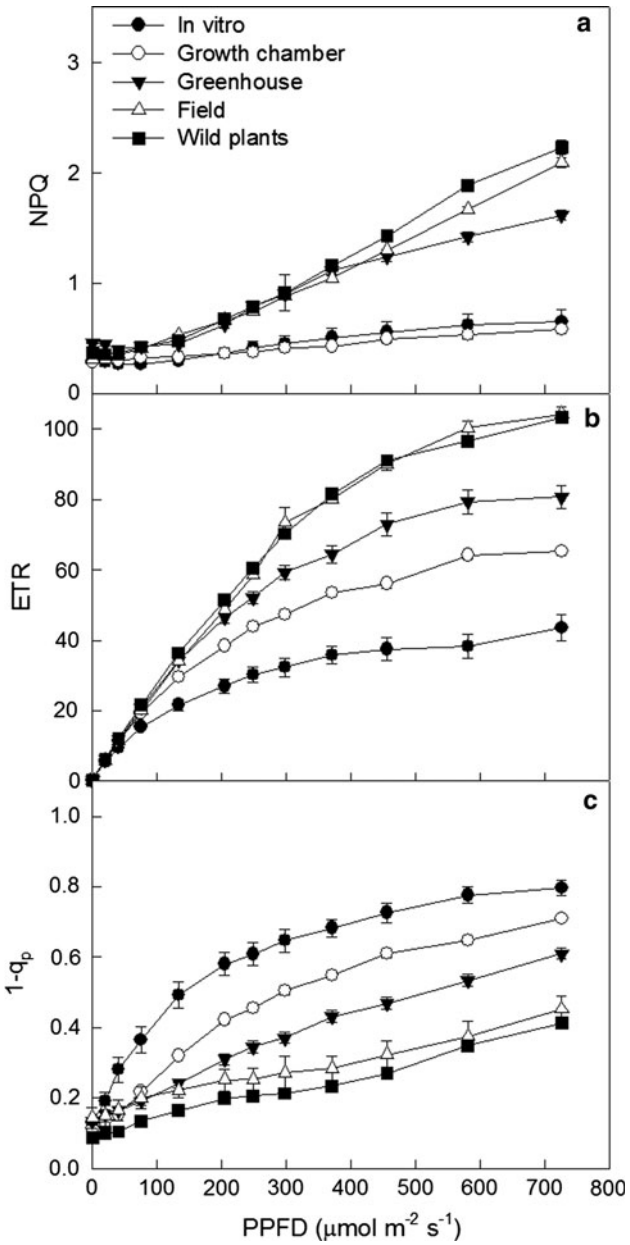

Fig. 6 Light responses in attached *T. major* leaves during acclimatization and in the field. **a** Non-photochemical quenching (NPQ); **b** electron transport rate (ETR); **c** excitation pressure ($1 - q_p$)

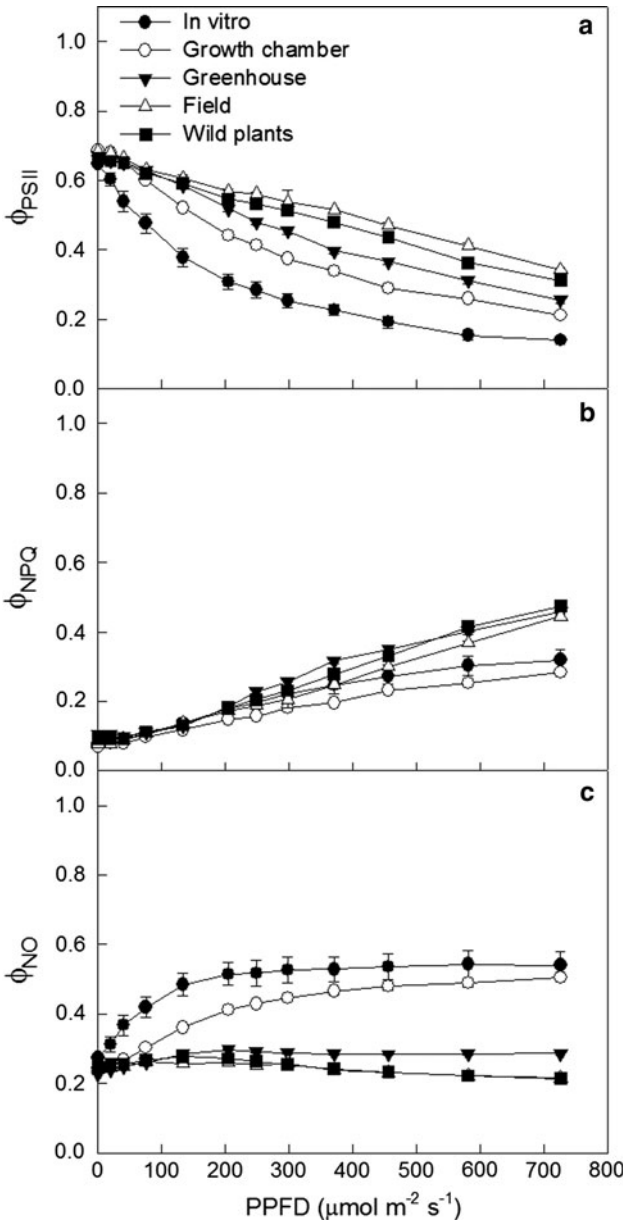

Fig. 7 Light responses of complementary PSII quantum yields in attached *T. major* leaves during acclimatization and in the field. **a** Quantum yield of photochemical energy conversion (ϕ_{PSII}); **b** quantum yield of regulated energy dissipation (ϕ_{NPQ}); **c** quantum yield of non-regulated energy dissipation (ϕ_{NO})

because g_s was higher in vitro and in growth chamber plants compared to other stages (Fig. 2a). However, the results clearly show that the stomatal control acquired during acclimatization is involved in the regulation of water loss to prevent uncontrolled wilting, as shown by the lower E values during the decline in relative humidity in the growth chamber (Fig. 2c). This suggests that the poor photosynthetic capacity of in vitro plants is responsible for their low or negative net photosynthetic rate. This is likely to reflect the low activity of RuBisCO, potentially through feedback inhibition caused by the accumulation of sucrose and starch (Piqueras et al. 1998; Genoud et al. 2000). The elevated C_i value (Fig. 2d) and the reasonable ETR value (Fig. 5c) in vitro also indicate that CO_2 assimilation is depressed at this stage, and that the absorbed electrons are used in alternative non-assimilatory electron transport processes to compensate for the restricted energy flux through the photosynthetic pathway. Given that large amounts of NO_3 are used in the culture medium, it is likely that part of the photosynthetic electron flow in vitro is used for the reduction of nitrates, which accumulate within the cultured plant cells (Triques et al. 1997).

Table 2 Total chlorophyll (Chl t), carotenoid (Car), anthocyanin and soluble protein (S-protein) contents during acclimatization, and chlorophyll/carotenoid ratio (Chl/Car) in the leaves of *T. major* plants

Acclimatization stage	Chl t (mg g_{Fw}^{-1})	Car (mg g_{Fw}^{-1})	Chl t/Car	Anthocyanins (mg g_{Fw}^{-1})	S-protein (mg g_{FW}^{-1})
In vitro	0.790 ± 0.161c	0.179 ± 0.038b	4.43 ± 0.04a	0.044 ± 0.010ab	29.39 ± 2.23ab
Growth chamber	1.767 ± 0.113b	0.417 ± 0.028a	4.24 ± 0.08a	0.069 ± 0.013a	20.8 ± 1.78b
Greenhouse	2.112 ± 0.020a	0.474 ± 0.023a	4.45 ± 0.04a	0.030 ± 0.009ab	36.84 ± 5.10a
Field	0.616 ± 0.019c	0.193 ± 0.003b	3.20 ± 0.13b	0.026 ± 0.010b	3.74 ± 1.13c
Wild plants	0.742 ± 0.056c	0.235 ± 0.012b	3.15 ± 0.11b	0.035 ± 0.006ab	1.05 ± 0.23c

Mean ± SE (n = 10) within each column with different letters are significantly different ($P < 0.05$) according to the SNK test

The physiological adjustments during acclimatization can be evaluated more accurately by Chl fluorescence measurements, either at a constant PPFD or in response to increasing PPFD (Alvarez et al. 2012). The F_v/F_m ratio, a sensitive and early indicator of photo-inhibition and changes in photochemical efficiency, remained approximately constant throughout acclimatization (Figs 3, 4), suggesting the photosynthetic machinery was stable. This ratio also fitted within the typical range expected for healthy and non-stressed plants, i.e. 0.75–0.85 (Björkman and Demmig 1987; Bolhár-Nordenkampf et al. 1989), as also reported for other species (Brito et al. 2009; Ďurkovič et al. 2010; Osório et al. 2012).

Although F_v/F_m remained steady, the F_m and F_0 values declined in both the regenerated and wild plants under field conditions (data not shown), probably reflecting changes in the optical properties of the leaf, which can modify the proportion of incident PPFD that is absorbed. As discussed above, the development of leaf hairs and the loss of chlorophyll are likely to reduce the absorbance capacity of the leaves thus enhancing photoprotection and the stability of the photosynthetic machinery. In contrast, the in vitro plants and those undergoing early acclimatization lacked such protective traits and were more susceptible to light, as indicated by the decline in photochemical efficiency (ϕ_{PSII}).

One of the best ways to study the processes that regulate photosynthesis and to evaluate the capacity of plants to cope with excess excitation energy is energy partitioning analysis (Kramer et al. 2004; Kornyeyev et al. 2006; Klughammer and Schreiber 2008; Osório et al. 2011). As shown in Fig. 4, the decaying ϕ_{PSII} values (particularly in vitro) were balanced by an increase in non-regulated energy dissipation (increasing ϕ_{NO}) rather than downregulation (invariable ϕ_{NPQ}), suggesting suboptimal photoprotection. However, the ϕ_{NO} value declined and the ϕ_{PSII} value increased throughout acclimatization, providing evidence for increasing photosynthetic performance. The ϕ_{NO} value is thought to reflect the portion of energy that is passively dissipated in the form of heat (constitutive loss) and fluorescence emission, mainly due to the closure of PSII reaction centers (Klughammer and Schreiber 2008). Indeed, the improvement of ϕ_{PSII} during acclimatization (134 μmol m^{-2} s^{-1}) resulted from the gradual reduction of the fraction of closed centers ($1 - q_p$) rather than changes to the excitation capture efficiency of open centers (F_v'/F_m') (Fig. 5a, b). This would support a hypothesis that the modulation of PSII excitation pressure during acclimatization reflects changes to the structure and function of the photosynthetic apparatus to prevent photo-inhibitory damage.

As expected, the evidence collected from light response curves (Figs 6, 7) showed that the pattern of energy partitioning changed according to the acclimatization stage. *T. major* plants in the field protected themselves against higher PPFD by increasing NPQ and ϕ_{NPQ}, indicating that regenerated plants in the field can adapt to cope with high PPFD in the same manner as wild plants. In contrast, the large increase in the ϕ_{NO} values observed in the in vitro and growth chamber plants confirmed that the photochemical energy conversion pathway and other regulatory mechanisms were insufficient to protect the plants from excess light, even though the mean ϕ_{NPQ} values increased with the PPFD (Calatayud et al. 2006). If these plants are transferred directly into the field without passing through an intermediate stage in the greenhouse, they would therefore be more prone to suffer from oxidative stress and could even die. This conclusion was also supported by the light-dependent responses of the electron transport rate and excitation pressure (Fig. 6).

In addition to light, drought also causes high mortality in micropropagated plants transferred to a natural environment, particularly in Mediterranean climates (low precipitation, intense illumination and high temperatures during the summer months). A wide range of environmental stresses (e.g. excess energy excitation, dehydration and temperature extremes) can induce the generation of reactive oxygen species (ROS), thereby disrupting the balance between production and metabolism and favoring the onset of oxidative stress (Neill et al. 2002). Usually, ROS are considered toxic cellular metabolites in plants, but H_2O_2 and others also act as signaling molecules that mediate responses to diverse stimuli (Foyer et al. 1997; Neill et al. 2002; Zhang et al. 2010; Vergara et al. 2012). The results

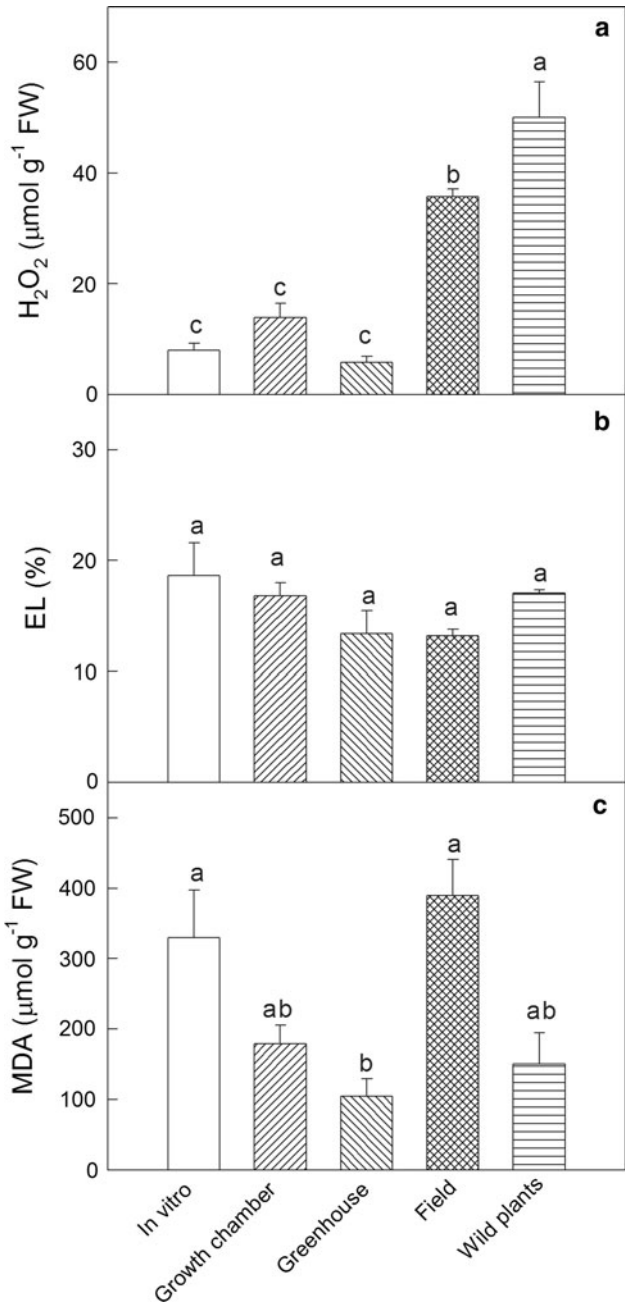

Fig. 8 Oxidative stress indicators in *T. major* leaves during acclimatization and in the field. **a** H_2O_2 concentration; **b** electrolyte leakage; **c** malondialdehyde concentration. Data represent mean ± SE (n = 5), and different letters are significantly different ($P < 0.05$) according to the SNK test

of this investigation showed that H_2O_2 levels are higher in the micropropagated and wild field plants than in others stages (Fig. 8a), potentially indicating a response to oxidative stress. However, acclimatization and field transfer did not increase electrolyte leakage, indicating no loss of membrane integrity (Fig. 8b) and thus robust tolerance under field conditions (Brito et al. 2009). Similarly, there was no difference in MDA levels between regenerated and wild plants, suggesting there was no increase in membrane damage caused by lipid peroxidation (Fig. 8c).

Recently, micropropagated *T. major* plants were shown to be protected against oxidative stress during drought and recovery under high temperatures, suggesting the plants are tolerant to these forms of stress (Osório et al. 2013). It is therefore possible that the increased production of H_2O_2 in the micropropagated and wild field plants is not a response to oxidative stress, but could instead represent an early signal leading to the modification of gene expression and the activation of antioxidant defense systems (Jiang and Zhang 2001).

Overall, the results of this investigation confirmed that the successful establishment of in vitro regenerated *T. major* plants in the field resulted from changes in their morphological and physiological characteristics, triggered by gradual acclimatization to the changing environment. The plasticity of those traits allows the species to cope with the environmental conditions in their natural habitat without a noticeable decline in photosynthetic competence and growth compared to wild plants. Therefore, the acclimatization procedure described herein, combined with the previously-reported micropropagation protocol, provides a promising technique for the conservation and restoration of depleted populations of *T. major*. This approach could be also used as a starting point for the acclimatization of other endangered species and their eventual establishment in the field.

Acknowledgments The authors M. L. Osório, S. Gonçalves and N. Coelho thank the Portuguese Foundation for Science and Technology for grants SFRH/BPD/35410/2007, SFRH/BPD/31534/2006 and SFRH/BD/63501/2009, respectively.

References

Alvarez C, Sáez P, Sáez K, Sánchez-Olate M, Ríos D (2012) Effects of light and ventilation on physiological parameters during in vitro acclimatization of *Gevuina avellana* mol. Plant Cell Tiss Organ Cult 110:93–101

Amâncio S, Rebordão JP, Chaves MM (1999) Improvement of acclimatization of micropropagated grapevine: photosynthetic competence and carbon allocation. Plant Cell Tiss Organ Cult 58:31–37

Bilz, M. (2011). Tuberaria major. In: IUCN 2012. IUCN red list of threatened species. Version 2012.2. www.iucnredlist.org

Björkman O, Demmig B (1987) Photon yield of O_2 evolution and chlorophyll fluorescence characteristics at 77 K among vascular plants of diverse origin. Planta 170:489–504

Bolhár-Nordenkampf HR, Long SP, Baker NR, Öquist G, Schreiber U, Lechner EG (1989) Chlorophyll fluorescence as a probe of the photosynthetic competence of leaves in the field: a review of current instrumentation. Funct Ecol 3:497–514

Bradford MM (1976) A rapid and sensitive method for the quantitation of microgram quantities of protein utilising the principle of protein dye binding. Anal Biochem 72:248–254

Brito G, Costa A, Coelho C, Santos C (2009) Large-scale field acclimatization of *Olea maderensis* micropropagated plants: morphologic and physiologic survey. Trees 23:1019–1031

Calatayud A, Roca D, Martinez PF (2006) Spatial-temporal variations in rose leaves under water stress conditions studied by chlorophyll fluorescence imaging. Plant Physiol Biochem 44:564–573

Chaves MM, Maroco JP, Pereira JS (2003) Understanding plant responses to drought-from genes to the whole plant. Funct Plant Biol 30:239–264

Demmig-Adams B (1998) Survey of thermal energy dissipation and pigment composition in sun and shade leaves. Plant Cell Physiol 39:474–482

Dijkstra P (1989) Cause and effect of differences in specific leaf area. In: Lambers H et al (eds) Causes and consequences of variation in growth rate and productivity of higher plants. Academic Publishing, the Hague, pp 125–140

Dŭrkovič J, Čanŏvá I, Priwitzer T, Biroščíková M, Kapral P, Saniga M (2010) Field assessment of photosynthetic characteristics in micro propagated and grafted wych elm (*Ulmus glabra* Huds.) trees. Plant Cell Tiss Organ Cult 101:221–228

Ehleringer JR, Mooney HA (1978) Leaf hairs: effects on physiological activity and adaptive value to a desert shrub. Oecologia 37:183–200

Foyer CH, Lopez-Delgado H, Dat JF, Scott IM (1997) Hydrogen peroxide and glutathione-associated mechanisms of acclamatory stress tolerance and signaling. Physiol Plant 100:241–254

Genoud C, Sallanon H, Hitmi A, Maziere Y, Coudret A (2000) Growth, stomatal conductance, photosynthetic rate, ribulose-1,5-bysphosphate carboxylase/oxydase and phosphoenolpyruvate carboxylase activities during root and acclimatization of *Rosa hybrida* plantlets. Photosynthetica 38:629–634

Genty B, Briantais JM, Baker NR (1989) The relationship between the quantum yield of photosynthetic electron transport and quenching of chlorophyll fluorescence. Biochim Biophys Acta 990:87–92

Gonçalves S, Fernandes L, Pérez-García F, González-Benito ME, Romano A (2009) Germination requirements and cryopreservation tolerance of seeds of the endangered species *Tuberaria major*. Seed Sci Technol 37:480–484

Gonçalves S, Fernandes L, Romano A (2010) High frequency in vitro propagation of the endangered species *Tuberaria major*. Plant Cell Tiss Organ Cult 101:359–363

Guan QZ, Guo YH, Sui XL, Li W, Zhang ZX (2008) Changes in photosynthetic capacity and antioxidant enzymatic systems in micropropagated *Zingiber officinale* plantlets during their acclimation. Photosynthetica 46:193–201

Hazarika BN (2006) Morpho-physiological disorders in vitro culture of plants. Sci Hortic 108:105–120

Hodges D, DeLong JM, Forney CF, Prange RK (1999) Improving the thiobarbituric acid-reactive-substances assay for estimating lipid peroxidation in plant tissues containing anthocyanin and other interfering compounds. Planta 207:604–611

Huang D, Dai W (2011) Direct regeneration from in vitro leaf and petiole tissues of *Populus tremula* 'Erecta'. Plant Cell Tiss Organ Cult 107:169–174

ICN (Instituto da Conservação da Natureza) (2006) Plano sectorial da rede natura. Flora: Tuberaria major (Willk.) P. Silva & Rozeira. http://www.icn.pt/psrn2000/caracterizacao_valores_naturais/flora/Tuberaria%20major.pdf. Accessed Dec 15, 2012

Jiang M, Zhang J (2001) Effect of abscisic acid on active oxygen species, antioxidative defence system and oxidative damage in leaves of maize seedlings. Plant Cell Physiol 42:1265–1273

Klughammer C, Schreiber U (2008) Complementary PS II quantum yields calculated from simple fluorescence parameters measured by PAM fluorometry and the Saturation Pulse method. PAM Appl Notes 1:27–35

Kornyeyev D, Logan BA, Tissue DT, Allen RD, Holaday AS (2006) Compensation for PSII photoinactivation by regulated non-photochemical dissipation influences the impact of photoinactivation on electron transport and CO_2 assimilation. Plant Cell Physiol 47:437–446

Kramer DM, Johnson G, Kiirats O, Edwards GE (2004) New fluorescence parameters for the determination of QA redox state and excitation energy fluxes. Photosynth Res 79:209–218

Kyparissis A, Petropoulou Y, Manetas Y (1995) Summer survival of leaves in a soft-leaved shrub (*Phlomis fructicosa* L., Labiatae) under Mediterranean field conditions: avoidance of photo inhibitory damage through decreased chlorophyll contents. J Exp Bot 46:1825–1831

Lichtenthaler HK (1987) Chlorophylls and carotenoids: pigments of photosynthetic biomembranes. Meth Enzymol 148:50–382

López IS, González FV, Lui GC (2006) Micropropagation of *Helianthemum inaguae*, a rare and endangered species from the Canary Islands. Bot Macaronésica 26:55–64

Loreto F, Velikova V (2001) Isoprene produced by leaves protects the photosynthetic apparatus against ozone damage, quences ozone products, and reduces lipid peroxidation of cellular membranes. Plant Physiol 127:781–787

Lutts SJ, Kinet M, Bouharmont J (1996) NaCl-induced senescence in leaves of rice (*Oriza sativa* L.) cultivar differing in salinity resistance. Ann Bot 78:389–398

Mancinelli AL (1984) Photoregulation of anthocyanin synthesis: VIII effects of light pretreatments. Plant Physiol 75:447–453

Munné-Bosch S, Alegre L (1999) Changes in carotenoids, tocopherols and diterpenes during drought and recovery, and the biological significance of chlorophyll loss in *Rosmarinus officinalis* plants. Planta 210:925–931

Murashige T, Shoog F (1962) A revised medium for rapid growth and bio-assays with tobacco tissue cultures. Physiol Plant 15: 473–497

Neill S, Desikan R, Clarke A, Hurst R, Hancock J (2002) Hydrogen peroxide and nitric oxide as signaling molecules in plants. J Exp Bot 53:1237–1247

Nicotra AB, Atkin OK, Bonser SP, Davidson AM, Finnegan EJ, Mathesius U, Poot P, Purugganan MD, Richards CL, Valladares F, van Kleunen M (2010) Plant phenotypic plasticity in a changing climate. Trends Plant Sci 15:684–692

Osório ML, Osório J, Vieira AC, Gonçalves S, Romano A (2011) Influence of enhanced temperature on photosynthesis, photooxidative damage, and antioxidant strategies in *Ceratonia siliqua* L. seedlings subjected to water deficit and rewatering. Photosynthetica 49:3–12

Osório ML, Osório J, Gonçalves S, David MM, Correia MJ, Romano A (2012) Carob trees (*Ceratonia siliqua* L.) regenerated in vitro can acclimatize successfully to match the field performance of seed-derived plants. Trees 26:1837–1846

Osório ML, Osório J, Romano A (2013) Photosynthesis, energy partitioning, and metabolic adjustments of the endangered Cistaceae species *Tuberaria major* under high temperature and drought. Photosynthetica 51:75–84

Oxborough K, Baker NR (1997) Resolving chlorophyll a fluorescence images of photosynthetic efficiency into photochemical and non-photochemical components: calculation of qP and F_v'/F_m' without measuring F_o'. Photosynth Res 54:135–142

Piqueras A, Van Huylenbroeck JM, Han BH, Debergh PC (1998) Carbohydrate partitioning and metabolism during acclimatization of micropropagated *Calathea*. Plant Growth Regul 26:25–31

Pospíšilová J, Tichá I, Kadleček P, Haisel D, Plzáková Š (1999) Acclimatization of micropropagated plants to ex vitro conditions. Biol Plant 42:481–497

Preece JE (2010) Acclimatization of plantlets from in vitro to the ambient environment. In: Wiley Encycl Ind Biotechnol, pp 1–9

Raju CS, Kathiravan K, Aslam A, Shajahan A (2013) An efficient regeneration system via somatic embryogenesis in mango ginger (*Curcuma amada* Roxb.). Plant Cell Tiss Organ Cult 112: 387–393

Siddique I, Anis M (2008) An improved plant regeneration system and *ex vitro* acclimatization of *Ocimum basilicum* L. Acta Physiol Plant 30:493–499

Triques K, Rival A, Beulé T, Puard M, Roy J, Nato A, Lavergne D, Havaux M, Verdeil JL, Sangare A, Hamon S (1997) Photosynthetic ability of in vitro grown coconut plantlets derived from zygotic embryos. Plant Sci 127:39–51

Vergara R, Parada F, Rubio S, Pérez FJ (2012) Hypoxia induces H_2O_2 production and activates antioxidant defence system in grapevine buds through mediation of H_2O_2 and ethylene. J Exp Bot 63:4123–4131

Yang L, Wang J, Bian L, Li Y, Shen H (2012) Cyclic secondary somatic embryogenesis and efficient plant regeneration in mountain ash (*Sorbus pohuashanensis*). Plant Cell Tiss Organ Cult 111:173–182

Zhang A, Zhang J, Ye N, Cao J, Tan M, Zhang J, Jiang M (2010) ZmMPK5 is required for the NADPH oxidase-mediated self propagation of apoplastic H_2O_2 in brassinosteroid-induced antioxidant defence in leaves of maize. J Exp Bot 61:4399–4411